Turkish J. Eng. Env. Sci.
31 (2007) , 211 – 223.

Computation of Time-Accurate Laminar Flows Using Dual Time Stepping and Local Preconditioning with Multigrid

Murat UYGUN
Department of Aeronautical Engineering, Turkish Air Force Academy İstanbul-TURKEY
e-mail: m.uygun@hho.edu.tr
Kadir KIRKKÖPRÜ
Department of Mechanical Engineering, İstanbul Technical University İstanbul-TURKEY

Received 14.11.2006

Abstract

A cell-centered finite volume method with explicit dual time-stepping and a low Mach number preconditioning technique is successfully applied to 2-dimensional Navier-Stokes equations for the numerical solution of time-dependent flows ranging from near incompressible limit to high subsonic Mach numbers. Preconditioning techniques have been widely used in order to remove the disparity between acoustic and convective speeds that degrades the convergence rate noticeably at low subsonic Mach numbers. In dual time stepping, a modified steady problem is solved by advancing in pseudo time at each physical time step. A multistage explicit Runge-Kutta time-stepping scheme is used for marching in pseudo time. Convergence is accelerated by means of local time stepping, residual smoothing, and multigrid. The accuracy of the time-accurate Navier-Stokes solver is verified by comparing predictions of the Strouhal numbers for the Karman vortex streets of the cylinder and of the blunt flat plate with the experimental data.

Key words: Dual time stepping, Local preconditioning, Laminar flow, Multigrid.

Introduction

The simulation of time accurate flows at all speeds is essential since many practical flows of engineering interest are inherently transient and may range from incompressible limit to supersonic speeds. It was common to exploit "pressure-based" schemes for the computation of incompressible flows and "density-based" schemes for compressible flows. Today, flow problems at all speeds can be handled by a well-assessed flow solver employing a single solution algorithm. A common practice for deriving a single solution algorithm from "density-based" schemes is to modify the Navier-Stokes equations via a low Mach number preconditioning technique. The low Mach number preconditioning technique resorts to multiplication of spatial derivatives by a suitable matrix in order to equalize the eigenvalues and hence to alleviate the stiffness occurring when the flow speed is very small in comparison to acoustic speed. However, preconditioning changes the original form of the governing equations and breaks down the time accuracy. Fortunately, time-accurate preconditioned governing equations can be solved by means of a dual time stepping approach (Jameson, 1991), where a modified steady problem is solved at each physical time step by advancing in pseudo time. In addition, the use of dual time stepping is beneficial in the computation of viscous flows, where the smaller time step is required for numerical stability due to high aspect ratio cells existing in the computational grid, since the use of dual time stepping allows the physical time step not to be limited by the corresponding values in the smallest cell and to be selected based on the numerical accuracy criterion. Acceleration techniques, such as local time stepping, implicit residual smoothing and multigrid, which are devised for steady flow computations, can be used to solve

the modified steady problem as well.

In previous studies, preconditioning was applied by adding a pseudo time derivative to the discrete equation and by multiplying it by the preconditioning matrix (Dailey and Pletcher, 1996; Vatsa and Turkel, 2003). In the current work, a new form of dual time stepping for preconditioned time-accurate governing equations is proposed. The resulting time stepping scheme has a simpler form, since it has considerably less matrix multiplication and no matrix inversion. It also provides the conditions taken into account in previous studies. The preconditioning matrix of Weiss and Smith (1995) is adopted. Convective terms are evaluated using a central differencing scheme (Jameson et al., 1981). The flux vectors at the midpoint of a cell face are computed by arithmetic averaging of flow variables at 2 neighboring cells. The variables required for the computation of viscous terms are also averaged at a cell face. Gradients at the midpoints of a cell face are computed by means of Green's theorem (Rizzi et al., 1993). Preconditioned time-dependent equations are integrated in pseudo time with a multistage explicit Runge-Kutta scheme. Convergence is accelerated by local time stepping (Arnone et al., 1995), residual smoothing (Jameson and Baker, 1983; Jameson, 1985a; Martinelli and Jameson, 1988) and multigrid. A multigrid method based on a Full Approximation Storage (FAS) scheme (Jameson, 1983; Jameson, 1985b; Martinelli et al., 1986) is used together with a Full Multigrid Algorithm (FMG) (Brandt, 1981).

The formulation, methodology, and validation are presented in order to prove the efficiency of the current flow solver for time-dependent flows. The first test case involves low Reynolds number flows past a cylinder at near incompressible and compressible low subsonic flows. The second test case involves high subsonic flow past a blunt flat plate. A sensitivity study is carried out including the effects of both grid density and physical time step. Grid and time step independent results are presented only. Predictions of the Strouhal numbers for the Karman vortex streets of the cylinder and of the blunt flat plate show good agreement with numerical solutions (Belov et al., 1995; Liu et al., 1998; Rogers and Kwak, 1990; Massey and Abdol-Hamid, 2003) and experimental data (Roshko, 1954; Willie, 1960; Heinemann et al., 1976; Schlichting, 1979).

Governing Equations

Navier-Stokes equations are written in integral form as

$$\iint_{\Omega} \frac{\partial \vec{C}}{\partial t} d\Omega + \oint_{\partial\Omega} \vec{F}\vec{n} dS = 0, \qquad (1)$$

where Ω denotes the control volume surrounded by the control surface $\partial\Omega$. $\vec{C}$ is the vector of conservative variables. $\vec{F}$ is the flux vector, which can be split into a convective part $\vec{F}_C$ and a viscous part $\vec{F}_V$ such that $\vec{F} = \vec{F}_C - \vec{F}_V$. $\vec{n} = n_x\vec{i} + n_y\vec{j}$ is the outward unit vector normal to the cell face $\partial\Omega$.

The coefficient of laminar viscosity μ_L is computed by the Sutherland formula. Assuming air as an ideal gas, the equation of state is used to calculate the pressure and temperature:

$$p = (\gamma - 1)\,\rho \left[E - \frac{u^2 + v^2}{2} \right], \quad T = \frac{p}{\rho R}. \qquad (2)$$

γ is the ratio of specific heats and R is the gas constant.

In the incompressible limit, the governing equations become stiff, since the convective speed is very small in comparison to acoustic speed. This can be shown by means of a condition number χ, which is defined as the ratio of the largest to the smallest convective eigenvalues of Eq. (1):

$$\chi = \frac{(\Lambda_C)_{\max}}{(\Lambda_C)_{\min}} = \frac{M+1}{M} \qquad (3)$$

When the condition number becomes large (i.e. when $M \to 0$), the wave propagation becomes less efficient, since while the fastest wave is moving by $(\Lambda_C)_{\max}$ the slowest wave moves by $(\Lambda_C)_{\min}$. In order to alleviate the stiffness, the governing equations are transformed into a new form, whose convective eigenvalues are equalized such that $\chi \approx 1$. The transformation and its effect on convective eigenvalues are shown with the aid of 1-dimensional Euler equations in quasilinear form (Blazek, 2005).

$$\frac{\partial \vec{W}}{\partial t} + A_C \frac{\partial \vec{W}}{\partial x} = 0, \qquad (4)$$

where A_C is the convective flux Jacobian. Transformation of Eq. (4) into a new form results in

$$T\frac{\partial \vec{Q}}{\partial t} + A_C T \frac{\partial \vec{Q}}{\partial x} = 0. \qquad (5)$$

$T = \partial\vec{W} \big/ \partial\vec{Q}$ is the transformation matrix.

$\vec{Q} = \begin{bmatrix} p & u & v & T \end{bmatrix}^T$ is the vector of primitive variables. The matrix T in front of the time derivative

is replaced by its modified form Γ such that (Mulas et al., 2002)

$$\frac{\partial \vec{Q}}{\partial t} + \Gamma^{-1} A_C T \frac{\partial \vec{Q}}{\partial x} = 0. \tag{6}$$

Transforming Eq. (6) from $\vec{Q}$ to $\vec{W}$ by means of $T^{-1} = \partial \vec{W} \Big/ \partial \vec{Q}$ results in a preconditioned system of equations:

$$\frac{\partial \vec{W}}{\partial t} + P A_C \frac{\partial \vec{W}}{\partial x} = 0. \tag{7}$$

P is the preconditioning matrix, which is defined as $P = T\Gamma^{-1}$. Convective eigenvalues of the preconditioned system are computed from the matrix PA_C. Γ must be selected such that the convective eigenvalues are equalized and $\chi \approx 1$. In this work, the matrix Γ, which is defined by Weiss and Smith (1995), is used:

$$\Gamma = \begin{bmatrix} \rho_P^m & 0 & 0 & 0 & \rho_T \\ \rho_P^m u & \rho & 0 & 0 & \rho_T u \\ \rho_P^m v & 0 & \rho & 0 & \rho_T v \\ \rho_P^m w & 0 & 0 & \rho & \rho_T w \\ H\rho_P^m - (1 - \rho h_P) & \rho u & \rho v & \rho w & H\rho_T + \rho h_T \end{bmatrix} \tag{8}$$

where $\rho_P,\ \rho_T,\ h_P,\ h_T$ are the derivatives of density and enthalpy with respect to pressure and temperature, respectively. Superscript m denotes for the modified term.

$$\rho_P^m = \frac{1}{u_r^2} - \frac{\rho_T}{\bar{\rho} h_T}, \tag{9}$$

where u_r is the reference velocity, which is defined as (Mulas et al., 2002)

$$u_r = \min\left[\max\left(\left\|\vec{V}\right\|, \frac{\mu_L}{\rho \Delta x}, \varepsilon\sqrt{\frac{\Delta p}{\bar{\rho}}}\right), c\right]. \tag{10}$$

Equation (10) states that the reference velocity is not allowed to go below local convection and diffusion velocities and the velocity based on local pressure gradient. Δx is the characteristic length of the cell. ε is a small number $\left(\approx 10^{-3}\right)$. c is the speed of sound. When the flow is supersonic, the preconditioning matrix becomes a unit matrix and the original form of Navier-Stokes equations is recovered locally. Matrices T, Γ^{-1}, P^{-1} and eigenvalues of the preconditioned system for flow of an ideal gas are presented in a previous work (Mulas et al., 2002).

Spatial Discretization

Following Eq. (7), preconditioned Navier-Stokes equations are written in integral form as

$$\iint_\Omega \frac{\partial \vec{C}}{\partial t} d\Omega + P \oint_{\partial\Omega} \vec{F} \vec{n} dS = 0, \tag{11}$$

The cell-centered finite volume method is used in order to solve Eq. (11). Computational domain is divided into quadrilateral control volumes (Figure 1). In the cell-centered scheme, flow quantities are associated with the center of a control volume. The finite volume method requires the evaluation of the convective and viscous fluxes, which are assumed to be constant along the individual cell face.

After writing Eq. (11) for all cells and employing the method of lines, where spatial and temporal terms are discretized separately, a system of first-order ODE is obtained (Jameson et al., 1981). Approximating the integrals with the mean value theorem, Eq. (11) for a particular cell becomes

$$\Omega_{I,J} \frac{d\vec{C}_{I,J}}{dt} = -\vec{R}\left(\vec{C}_{I,J}\right), \tag{12}$$

where $\vec{R}\left(\vec{C}_{I,J}\right)$ is called the "residual," which is defined as

$$\vec{R}\left(\vec{C}_{I,J}\right) = P_{I,J} \sum_{ncf=1}^{4} \left(\vec{F}_C - \vec{F}_V\right)_{ncf} (\vec{n}\Delta S)_{ncf}. \tag{13}$$

I and J locate the particular cell and ncf identifies cell faces. ΔS is the area of the cell face. In regions where viscous effects are negligible, physical diffusion is not adequate to prevent odd-even decoupling of the cell-centered schemes. In order to remove odd-even decoupling of the solution and oscillations near shocks, stagnation points and boundary layer edges, the artificial dissipation term $\vec{D}$ is added to Eq. (13):

$$\vec{R}\left(\vec{C}_{I,J}\right) = P_{I,J} \sum_{ncf=1}^{4} \left[\left(\vec{F}_C - \vec{F}_V\right)\vec{n}\Delta S - \vec{D}_{I,J}\right]_{ncf}. \tag{14}$$

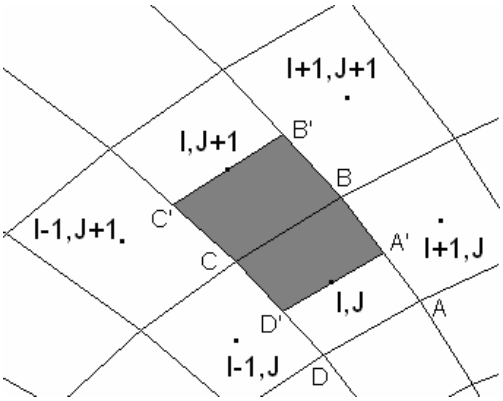

Figure 1. Control volume (cell), control surface (cell face) and auxiliary control volume.

The net dissipation flux through the faces of a particular cell is calculated as (Jameson et al., 1981)

$$\sum_{ncf=1}^{4} \vec{D} = \vec{D}_{I+1/2,J} - \vec{D}_{I-1/2,J} + \vec{D}_{I,J+1/2} - \vec{D}_{I,J-1/2}. \tag{15}$$

The dissipation flux at the cell face AB (Figure 1) is defined as

$$\vec{D}_{I+1/2,J} = \alpha_{I+1/2,J} P^{-1}_{I+1/2,J} \left(\varepsilon^{(2)}_{I+1/2,J} \delta^{(1)}_I \vec{C}_{I,J} - \varepsilon^{(4)}_{I+1/2,J} \delta^{(3)}_I \vec{C}_{I,J} \right), \tag{16}$$

where

$$P^{-1}_{I+1/2,J} = \left(P^{-1}_{I,J} + P^{-1}_{I+1,J} \right) \Big/ 2. \tag{17}$$

$\delta^{(1)}$ and $\delta^{(3)}$ are 1^{st} and third-order difference operators, respectively. $\varepsilon^{(2)}$ and $\varepsilon^{(4)}$ are the coefficients of second and fourth difference types, respectively. α is a scaling factor, which is written for I direction as (Blazek, 1994)

$$\alpha_{I+1/2,J} = \left[\left(\Lambda^I_c\right)_{I,J} + \left(\Lambda^I_c\right)_{I+1,J} \right] \Big/ 2, \tag{18}$$

where

$$\Lambda^I_C = \left[\frac{\left(M_r^2+1\right)}{2} \left| \vec{V}\vec{n} \right| + \frac{1}{2} \sqrt{ \left(\vec{V}\vec{n} \right)^2 \left(M_r^2-1\right)^2 + 4u_r^2 } \right] \Delta S^I. \tag{19}$$

Λ_C is the spectral radius of the convective flux Jacobian. $M_r = u_r/c$ is the reference Mach number and c is the local speed of sound.

Convective fluxes are evaluated by means of a central differencing scheme (Jameson et al., 1981). The total flux at the cell face AB (Figure 1) is approximated by

$$(\vec{F}\vec{n}\Delta S)_{I+1/2,J} = [\vec{F}_C(\vec{C}_{I+1/2,J}) - \vec{F}_V(\vec{U}_{I+1/2,J})](\vec{n}\Delta S)_{I+1/2,J}, \tag{20}$$

where

$$\vec{C}_{I+1/2,J} = \left(\vec{C}_{I,J} + \vec{C}_{I+1,J} \right) \Big/ 2 \text{ and } \vec{U}_{I+1/2,J} = \left(\vec{U}_{I,J} + \vec{U}_{I+1,J} \right) \Big/ 2 \tag{21}$$

$\vec{U}$ represents the flow variables $\tilde{u}, \tilde{v}, \bar{k}, \bar{\mu}$, which are required for the computation of the viscous terms and of the stresses. Gradients at the midpoint of the cell face BC are evaluated using Green's theorem with the aid of an auxiliary control volume Ω^{BC} (Figure 1), which is defined by the curve $A'B'C'D'$ (Rizzi et al., 1993). The derivative of temperature with respect to y coordinate is calculated as

$$\left(\frac{\partial T}{\partial y} \right)_{BC} = \frac{1}{\Omega^{BC}} \iint_{\Omega} \left(\frac{\partial T}{\partial y} \right) d\Omega = \frac{1}{\Omega^{BC}} \int_{\partial\Omega} T dS^{BC}_y \approx \frac{1}{\Omega^{BC}} \sum_{ncf=1}^{4} \left(T \Delta S^{BC}_y \right)_{ncf}, \tag{22}$$

where

$$\Omega^{BC} = \frac{1}{2} \left(\Omega_{I,J} + \Omega_{I,J+1} \right). \tag{23}$$

Temperature at cell faces is obtained as cell-centered values. The use of Eq. (22) yields a second-order accurate scheme for smoothly stretched grids.

Time Stepping

Equation (7) states that preconditioning requires the multiplication of spatial derivatives by the matrix P. This changes the original form of the governing equations and breaks down the time accuracy. Fortunately, time-accurate preconditioned equations can be solved by means of dual time stepping approach (Jameson, 1991). In previous studies, preconditioning was applied by adding a pseudo time derivative to the left-hand side of the discrete equation and by multiplying it by the matrix P^{-1} (Dailey and Pletcher, 1996; Vatsa and Turkel, 2003);

$$\Omega_{I,J} P^{-1}_{I,J} \frac{d\vec{C}_{I,J}}{d\tau} + \Omega_{I,J} \frac{d\vec{C}_{I,J}}{dt} = -\vec{R}\left(\vec{C}_{I,J} \right), \tag{24}$$

where

$$\vec{R}\left(\vec{C}_{I,J}\right) = \sum_{ncf=1}^{4}\left[\left(\vec{F}_C - \vec{F}_V\right)\vec{n}\Delta S - \vec{D}_{I,J}\right]_{ncf}. \tag{25}$$

τ is the pseudo time. Discretizing Eq. (24) with second-order time accurate, 3 point backward difference formula (BDF) for the physical time derivative and with first-order accurate BDF for the pseudo time derivative results in

$$\Omega_{I,J}\left(\frac{\vec{C}_{I,J}^{k+1} - \vec{C}_{I,J}^{k}}{\Delta\tau_{I,J}}\right) = -P_{I,J}\vec{R}^*\left(\vec{C}_{I,J}^{n+1}\right), \tag{26}$$

where

$$\vec{R}^*\left(\vec{C}_{I,J}^{n+1}\right) = \vec{R}\left(\vec{C}_{I,J}^{n+1}\right) + \frac{3\Omega_{I,J}}{2\Delta t}\vec{C}_{I,J}^{n+1} - \vec{Q}_{I,J}. \tag{27}$$

$\vec{R}^*$ is called the unsteady residual. The superscripts indicate time level. $\vec{Q}_{I,J}$ involves the terms that are invariant through the time stepping:

$$\vec{Q}_{I,J} = \frac{\Omega_{I,J}}{2\Delta t}\left(4\vec{C}_{I,J}^{n} - \vec{C}_{I,J}^{n-1}\right) \tag{28}$$

Time stepping in Eq. (26) is carried out using the M-stage Runge-Kutta (R-K) scheme, which is given as

$$\begin{array}{l}
\vec{C}_{I,J}^{(0)} = \vec{C}_{I,J}^{(k)} \\
\vdots \\
\left(I + \alpha_m \frac{3}{2}\frac{\Delta\tau_{I,J}}{\Delta t}P_{I,J}\right)\vec{C}_{I,J}^{(m)} = \vec{C}_{I,J}^{(0)} - \\
\alpha_m \frac{\Delta\tau_{I,J}}{\Omega_{I,J}}P_{I,J}\vec{R}^*\left(\vec{C}_{I,J}^{(m-1)}\right) + \alpha_m \frac{3}{2}\frac{\Delta\tau_{I,J}}{\Delta t}P_{I,J}\vec{C}_{I,J}^{(m-1)} \\
\vdots \\
\vec{C}_{I,J}^{(k+1)} = \vec{C}_{I,J}^{(M)}
\end{array}, \tag{29}$$

where $m = 1, 2, ...M$. I is the identity matrix. Solution of Eq. (29) requires performing 3 matrix multiplications and 1 matrix inversion at each R-K stage.

In this work, preconditioning is applied by adding a pseudo time derivative to the left-hand side of Eq. (12):

$$\Omega_{I,J}\frac{d\vec{C}_{I,J}}{d\tau} + \Omega_{I,J}\frac{d\vec{C}_{I,J}}{dt} = -\vec{R}\left(\vec{C}_{I,J}\right), \tag{30}$$

where

$$\vec{R}\left(\vec{C}_{I,J}\right) = P_{I,J}\sum_{ncf=1}^{4}\left[\left(\vec{F}_C - \vec{F}_V\right)\vec{n}\Delta S - \vec{D}_{I,J}\right]_{ncf}. \tag{31}$$

Discretizing Eq. (30) with second-order time accurate, 3 point BDF for the physical time derivative and with first-order accurate BDF for the pseudo time derivative results in

$$\Omega_{I,J}\left(\frac{\vec{C}_{I,J}^{k+1} - \vec{C}_{I,J}^{k}}{\Delta\tau_{I,J}}\right) = -\vec{R}^*\left(\vec{C}_{I,J}^{n+1}\right). \tag{32}$$

$\vec{R}^*$ has the same form as that given in Eq. (27), whereas the residual $\vec{R}$ is calculated by Eq. (31). Using the M-stage Runge-Kutta (R-K) scheme with the point-implicit calculation of the unsteady terms (Melson et al., 1993), the explicit time stepping reads

$$\begin{array}{l}
\vec{C}_{I,J}^{(0)} = \vec{C}_{I,J}^{(k)} \\
\vdots \\
\vec{C}_{I,J}^{(m)}\left(1 + \alpha_m\beta\frac{3}{2}\frac{\Delta\tau_{I,J}}{\Delta t}\right) = \vec{C}_{I,J}^{(0)} - \\
\alpha_m \frac{\Delta\tau_{I,J}}{\Omega_{I,J}}\vec{R}^*\left(\vec{C}_{I,J}^{(m-1)}\right) + \alpha_m\beta\frac{3}{2}\frac{\Delta\tau_{I,J}}{\Delta t}\vec{C}_{I,J}^{(m-1)} \\
\vdots \\
\vec{C}_{I,J}^{(k+1)} = \vec{C}_{I,J}^{(M)}
\end{array} \tag{33}$$

where $m = 1, 2, ...M$. $\beta \geq 2$ is adopted to stabilize the scheme (Venkatakrishnan and Mavriplis, 1996).

The use of dual time stepping proposed in Eq. (33) is advocated by 3 issues. First, as stated in Eq. (7), the multiplication of P by spatial derivatives only is sufficient to equalize the convective eigenvalues. Second, for both time stepping schemes presented in Eq. (29) and Eq. (33), pseudo time steps are calculated using the same matrix, which is obtained from the multiplication of the preconditioning matrix by convective flux Jacobian. Third, regarding the time stepping in Eq. (29), Vatsa and Turkel (2004) suggest turning off the preconditioning in the update stage and including the effect of preconditioning only in the artificial dissipation, in case the physical time step is sufficiently small. As can be seen in Eq. (33), the proposed time stepping scheme satisfies their suggestion by itself and requires no further treatment. Moreover, Eq. (33) has a simpler form than Eq. (29), since it has only 2 matrix multiplications (one for scaling artificial dissipation and the other for equalizing eigenvalues) and no matrix inversion at each R-K stage. Table 1 presents optimized Runge-Kutta coefficients for maximum stability of a centrally discretized scheme (Vatsa and Turkel, 2004).

Table 1. Optimized stage coefficients.

Central Differencing Scheme					
m	1	2	3	4	5
α	0.25	0.18	0.40	0.51	1.00

The convergence rate of the explicit time-stepping scheme is accelerated by local time stepping (Arnone et al., 1995) and residual smoothing (Jameson and Baker, 1983; Jameson, 1985a; Martinelli and Jameson, 1988) and multigrid. A multigrid method based on a Full Approximation Storage (FAS) scheme (Jameson, 1983; Jameson, 1985b; Martinelli et al., 1986) was implemented together with a Full Multigrid Algorithm (FMG) (Brandt, 1981). In this work, a V-cycle procedure with 3 grid levels is used to execute the multigrid strategy. The preconditioned residuals are used throughout the process. One Runge-Kutta time step before the restriction and no Runge-Kutta time step after prolongation are done on a fine grid. Robustness of the multigrid scheme is improved by performing 2 Runge-Kutta time steps on the coarse grid, and 3 on all coarser grids. Residuals and flow variables are restricted from fine to coarse grid by a weighted average. A forcing function is introduced into the time-stepping scheme. Solution corrections are prolongated from coarse to fine grid by bilinear interpolation. Implicit smoothing of solution corrections with constant coefficients is used in order to damp the high frequency errors, which are introduced by interpolation of the solution corrections. The FMG method is applied to provide an initial solution for the fine grid. The artificial dissipation model with constant coefficient, second-order differences is used on the coarse grids to reduce computational effort. The same Courant-Friedrichs-Lewy (CFL) number is used on all grids so that larger time steps are used on coarser grids. The viscous terms in Navier-Stokes equations are computed on coarse grids too.

Boundary Conditions

Boundary conditions on all grid levels are treated in the same way. Two layers of ghost cells are utilized. The velocity components are zero (no slip) at the solid wall. The wall pressure is obtained by extrapolation from the interior domain. The normal derivative of temperature is zero (adiabatic wall). A continuity condition is enforced along the wake cut. A characteristic boundary condition is applied to farfield boundaries (Vatsa and Turkel, 2004).

Computational Results

The numerical results given here demonstrate the accuracy and computational efficiency of the present preconditioned Navier-Stokes solver for the computation of time-accurate laminar flows. Test cases for the accuracy assessment are the flows past a circular cylinder and past a blunt flat plate. For both cases, the flow is in the laminar regime and started from steady conditions. Multigrid calculations are first done on coarse grid level to speed up the vortex shedding instability, and then fine grid computations are performed with a smaller time step. A V-cycle procedure with 3 grid levels is used in all computations in order to execute the multigrid strategy. The induced vortices are shed from upper and lower surfaces successively, resulting in the well-known Karman vortex street. The Strouhal number, which is a dimensionless frequency, is given by $St = f\,(D/U)$, where $D$is the diameter, $U$is the free stream velocity, and $f$is the frequency of the vortex shedding. For both test cases, a sensitivity study is carried out including the effects of both grid density and physical time step. Grid and time step independent results are presented only. The convergence criterion in pseudo time is based on L2 norm of density and was set to 10^{-4}. Computations were done on a PC with 1 Gbyte memory, operating Windows XP.

Flow past a circular cylinder

Near incompressible (M = 0.05 and M = 0.1) and compressible (M = 0.3) low subsonic flows past a circular cylinder are studied first. For all cases, the Reynolds number, which is based on the free-stream velocity and the cylinder diameter, is 200. A physical time step, which corresponds to about 50 steps for each period of vortex shedding, is used to obtain time independent solutions. A smaller physical time step results in a faster convergence rate in pseudo time. Larger time steps fail to resolve flow properties. An O-type computational grid with 256 × 128 cells is used in all computations (Figure 2). The spacing between the first grid point and the solid surface is 0.002D. The farfield boundary is located 20 diameters away from the cylinder.

Figures 3a-d present a typical convergence history and the time evolution of aerodynamic forces. Figure 4a presents the convergence rates in pseudo time for preconditioned and non-preconditioned schemes. When a small physical time step is used,

preconditioning does not improve the convergence rate significantly, since the CPU time required for a pseudo time step gained due to preconditioning is not significant in comparison to the non-preconditioned scheme. However, the numerical accuracy is improved, since the artificial dissipation is scaled. The gain in overall computational time may be improved, if the residual is to be reduced more than 4 levels.

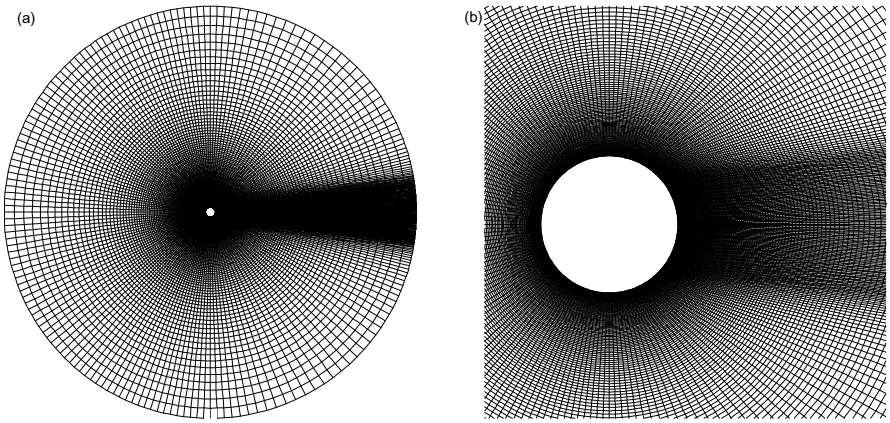

Figure 2. Computational grid (a) global view (b) close-up view.

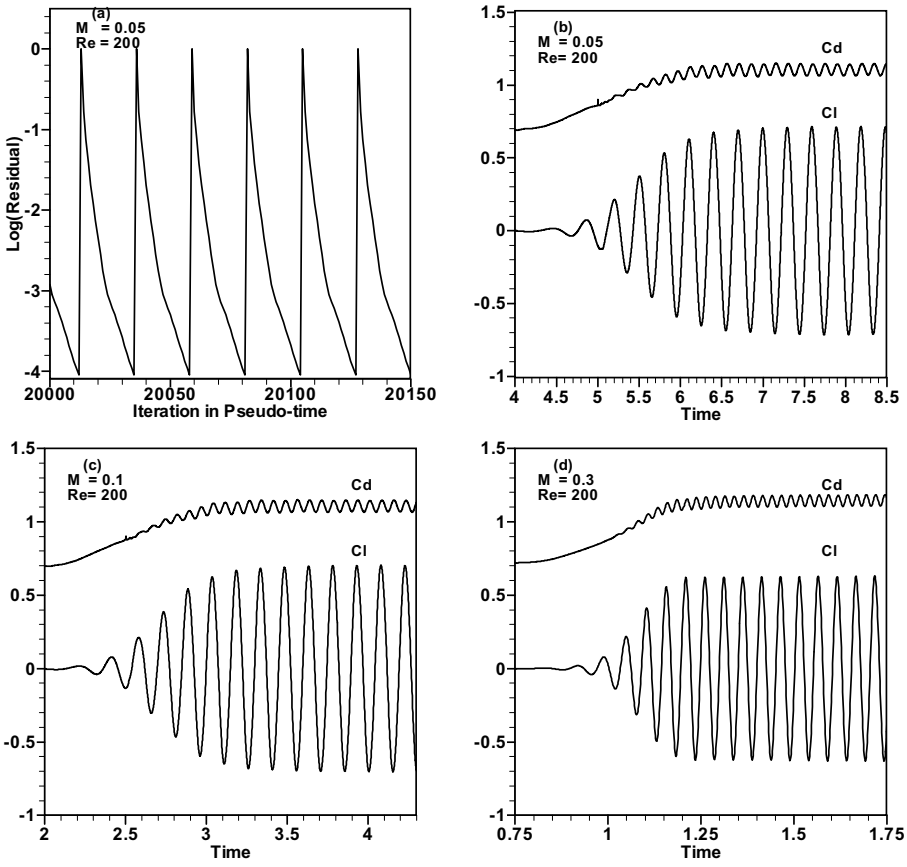

Figure 3. Typical convergence rate and time evolution of aerodynamic forces.

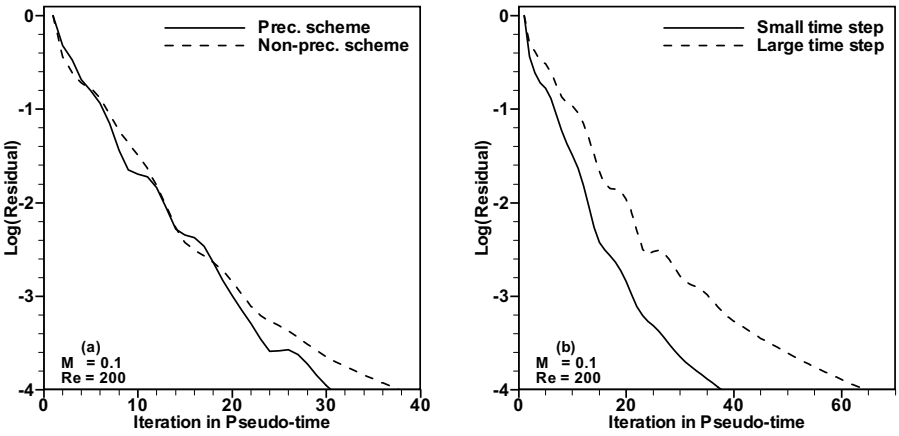

Figure 4. Convergence rates in a physical time step.

Table 2. Comparison of results, Re = 200.

		Present	Belov et al.	Liu et al.	Rogers et al.	Wille (Exp.)
Strouhal Number	M = 0.05	0.197	0.193	0.192	0.185	0.19
	M = 0.1	0.194				
	M = 0.3	0.192				
Cl	M = 0.05	±0.701	±0.64	±0.69	±0.65	
	M = 0.1	±0.665				
	M = 0.3	±0.639				
Cd	M = 0.05	1.11 ± 0.04	1.19 ±0.042	1.31 ±0.049	1.23 ±0.050	1.30
	M = 0.1	1.11 ± 0.041				
	M = 0.3	1.15 ± 0.04				

Figure 4b presents the convergence rates of the preconditioned scheme in pseudo time for small and large time steps. A large time step is obtained by doubling the small time step. A smaller physical time step results in a faster convergence rate in pseudo time. Isomach contours during 1 cycle of the Karman vortex shedding are plotted in Figure 5. t/T = 0 and t/T = 1 correspond to the locations in time where a maximum value of lift is calculated. The computed Strouhal number and aerodynamic coefficients agree with numerical solutions and experimental data given in Table 2. As the Mach number decreases, the Strouhal number and lift slightly increase.

Flow past a blunt flat plate

The capability of the present solver for handling wide range of flow speeds is assessed by calculating from low subsonic (M = 0.43) to high subsonic (M = 0.8) compressible flows past a flat plate. The flat plate has end caps, whose diameter is 1 m. The ratio of diameter to plate length including end caps is 0.03. An O-type computational grid with 680 × 192 cells is used in all computations (Figure 6).

Table 3. Comparison of results.

Strouhal Num.	$M_\infty = 0.43$	$M_\infty = 0.61$	$M_\infty = 0.80$
	$Re_l = 5.3x10^5$	$Re_l = 6.5x10^5$	$Re_l = 7.5x10^5$
Present	0.193	0.185	0.172
Massey et al.	0.246	0.211	0.190
Heinemann et al. (Exp.)	0.196	0.189	0.178

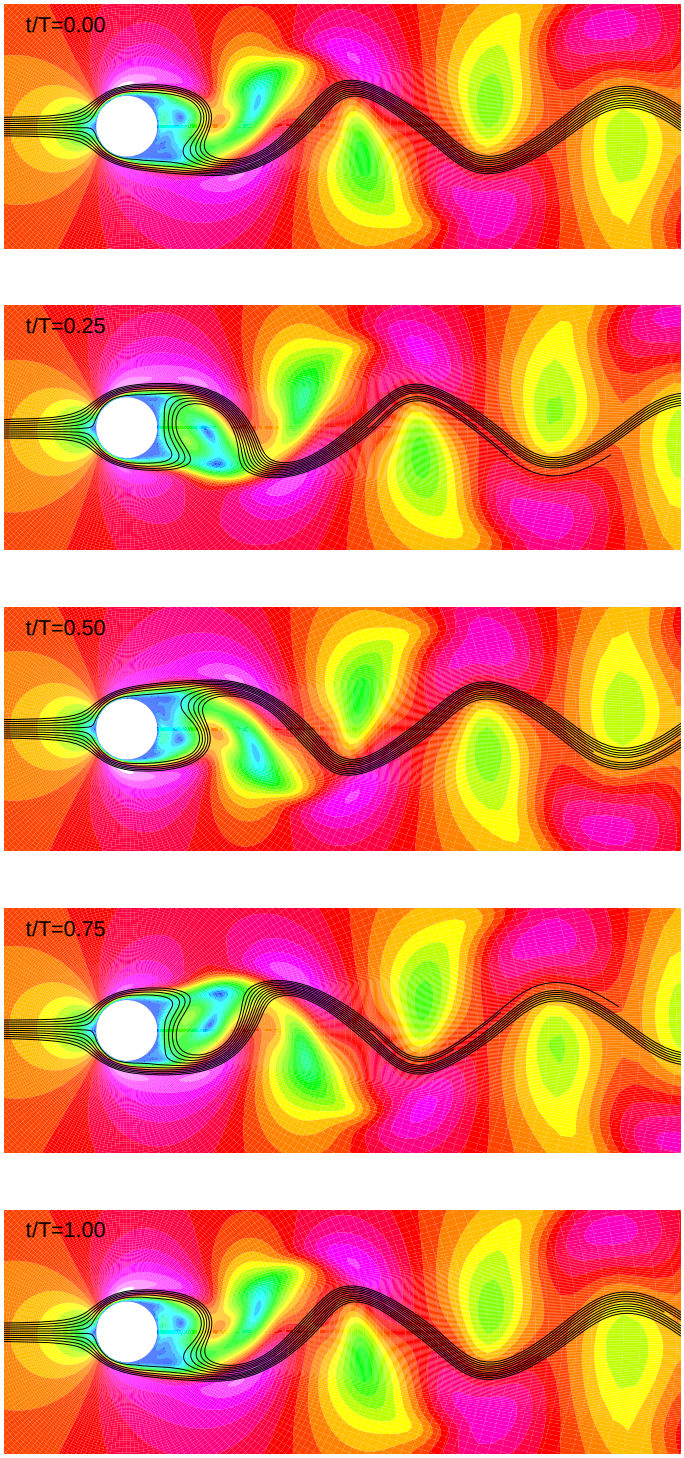

Figure 5. Isomach contours during one cycle of the Karman vortex shedding (M = 0.1, Re = 200).

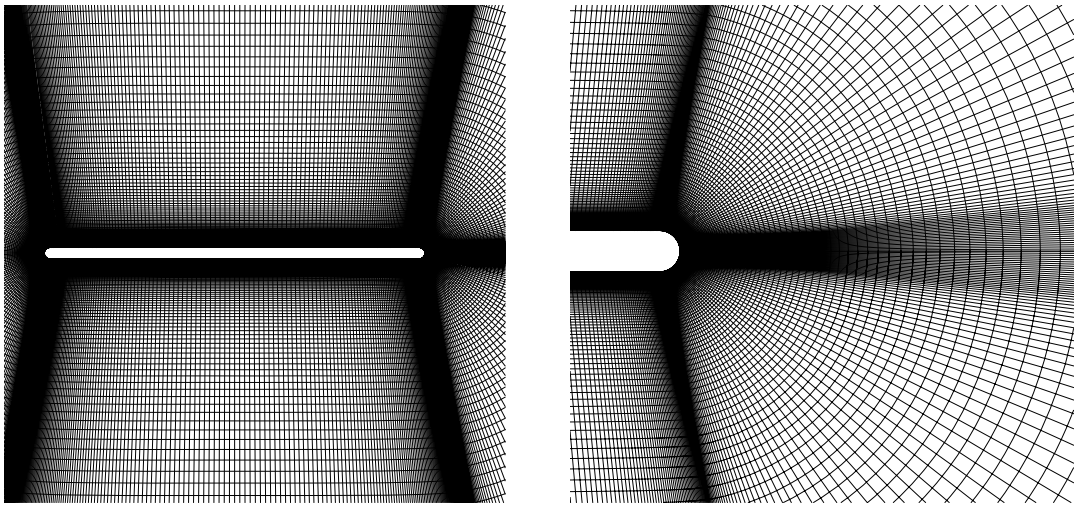

Figure 6. Computational grid (close-up view).

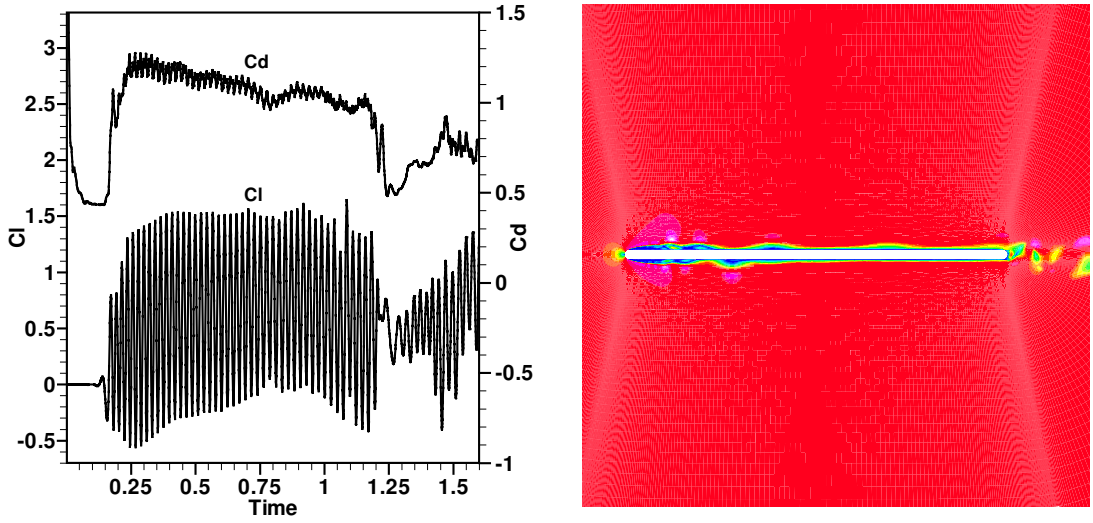

Figure 7. Aerodynamic forces and isomach contours past a flat plate (M = 0.61).

The spacing between the first grid point and the solid surface is 0.001D. The farfield boundary is located at a distance of 15 plate lengths. A physical time step, which corresponds to about 70 steps for each period of vortex shedding, is used to obtain time independent solutions. Table 3 presents the Reynolds numbers, which are based on the free-stream velocity and the plate length. Predictions of the Strouhal numbers agree well with the experimental data (Heinemann, 1976). Figures 7 and 8 indicate the isomach contours. The fore and aft separation and vortex street formation are evident and they agree with the simulated Schlieren experimental results presented by Massey and Abdul-Hamid (2003). Although a coarser grid is used here, calculated Strouhal numbers are in better agreement with experimental data in comparison to those calculated by Massey and Abdul-Hamid (2003).

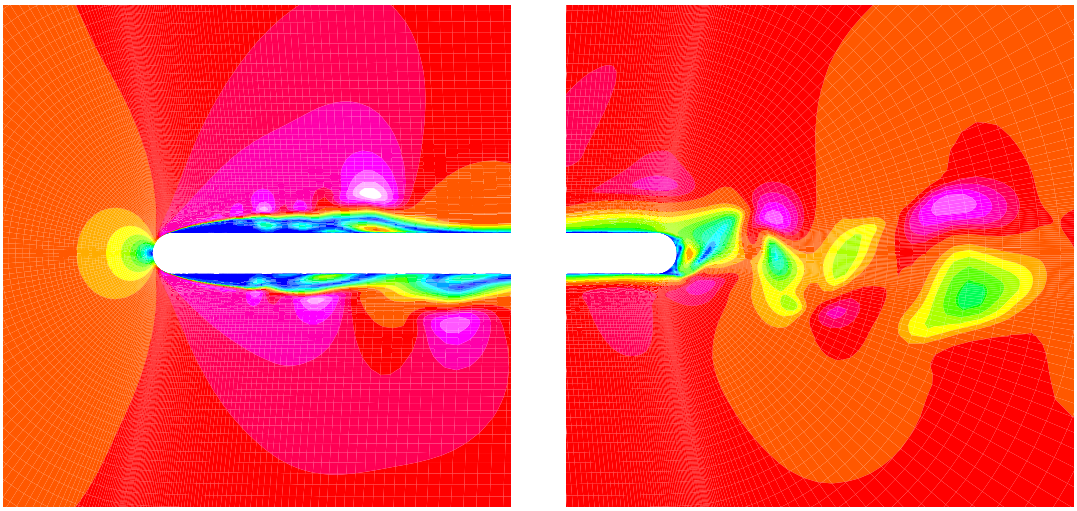

Figure 8. Isomach contours at leading and trailing edges (M = 0.61).

Conclusions

The capability of an existing density based solver, which incorporates a low Mach number preconditioning and dual time stepping method to accurately calculate time-accurate flows at wide range of Mach numbers, was investigated. The present code implements a proposed time stepping scheme and works efficiently in solving near incompressible as well as compressible subsonic flows with time accuracy. Computational results agree well with the experimental data. When the physical time step is sufficiently small, the preconditioning technique does not improve the convergence significantly. However, the solution accuracy is improved owing to scaled artificial dissipation. The CPU time per pseudo time step for the preconditioned scheme is almost the same as that for the non-preconditioned one.

Acknowledgment

The authors wish to thank Dr. Steven Massey from Eagles Aeronautics, Inc., USA, for his helpful input.

Nomenclature

$\vec{C}$	vector of conservative variables;
c	speed of sound;
$\vec{D}$	dissipation flux vector;
D	cylinder diameter;
f	frequency of vortex shedding;
$\vec{F}$	flux vector;
$\vec{F}_C$	convective flux vector;
$\vec{F}_V$	viscous flux vector;
$\vec{i}, \vec{j}$	unit vectors associated with the cartesian coordinates;
M_r	reference Mach number;
$\vec{n}$	outward unit normal vector;
p	pressure;
ρ	density;
R	gas constant;
$\vec{R}$	residual;
$\vec{R}^*$	unsteady residual;
T	temperature, transformation matrix;
u, v	velocity components;
x, y	cartesian coordinates;
t	physical time;
P	preconditioning matrix;
$\vec{Q}$	source vector, vector of primitive variables;
u_r	reference velocity;
$\vec{V}$	velocity vector;
α	scaling factor, stage coefficient of Runge-Kutta time stepping;
β	constant parameter;
$\delta^{(1)}, \delta^{(3)}$	first- and third-order difference operators;
ΔS	face area;
Δt	physical time step;
$\partial\Omega$	control surface;
Γ	modified form of the transformation matrix;
γ	ratio of specific heats;
$\varepsilon^{(2)}$	coefficient for artificial dissipation of second difference type;

$\varepsilon^{(4)}$ coefficient for artificial dissipation of fourth difference type;
μ viscosity coefficient;
Ω control volume.

Superscripts

I, J cartesian coordinate directions;
k pseudo time step counter;
n physical time step counter;
$*$ unsteady terms.

Subscripts

C, V convective and viscous terms;
I, J cell indices;
L laminar quantity;
m stage number in Runge-Kutta time stepping.

References

Arnone, A., Liou, M.S. and Povinelli, L.A., "Integration of Navier-Stokes Equations Using Dual Time Stepping and a Multigrid Method," AIAA Journal, 33, 985-990, 1995.

Belov, A., Martinelli, L., Jameson, A., "A New Implicit Algorithm with Multigrid for Unsteady Incompressible Flow Calculations," AIAA 95-0049, 1995.

Blazek, J., "Verfahren zur Beschleunigung der Lösung der Euler- und Navier-Stokes Gleichungen bei stationaren Über- und Hyperschallströmungen," PhD Thesis, University of Braunschweig, Germany, 1994.

Blazek, J., "Computational Fluid Dynamics: Principles and Applications," Elsevier, Oxford, 2005.

Brandt, A., "Guide to Multigrid Development, Multigrid Methods I," Lecture Notes in Mathematics, 960, Springer Verlag, New York, 1981.

Dailey, L.D. and Pletcher, R.H., "Evaluation of Multigrid Acceleration for Preconditioned Time-Accurate Navier-Stokes Algorithms," Computers & Fluids, 25, 791-811, 1996.

Heinemann, H., Lawaczeck, O. and Bütefisch, K.A., "Karman Vortices and Their Frequency Determination in the Wakes of Profiles in the Sub- and Transonic Regime," Symposium Transsonicum II Göttingen, 75-82, 1976.

Jameson, A., Schmidt, W. and Turkel, E., "Numerical Solutions of the Euler Equations by Finite Volume Methods Using Runge-Kutta Time-Stepping Schemes," AIAA Paper 81-1259, 1981.

Jameson, A. and Baker, T.J., "Solution of the Euler Equation for Complex Configurations," AIAA Paper 83-1929, 1983.

Jameson, A., "Solution of the Euler Equations for Two-dimensional, Transonic Flow by a Multigrid Method," Applied Mathematics and Computation, 13, 327-356, 1983.

Jameson, A., "Transonic Flow Calculations," Lecture Notes in Mathematics, 1127, 156-242, 1985a.

Jameson, A., "Multigrid Algorithms for Compressible Flow Calculations," Mechanical and Aerospace Engineering Report 1743, Princeton University, 1985b.

Jameson, A.; "Time Dependent Calculations Using Multigrid with Application to Unsteady Flows past Airfoils and Wings," AIAA Paper 91-1596, 1991.

Liu, C., Zheng, X. and Sung, C.H., "Preconditioned Multigrid Methods for Unsteady Incompressible Flows," Journal of Computational Physics, 139, 35-57, 1998.

Martinelli, L., Jameson, A. and Grasso, F., "A Multigrid Method for the Navier-Stokes Equations," AIAA 86-0208, 1986.

Martinelli, L. and Jameson, A., "Validation of a Multigrid Method for the Reynolds Averaged Equations," AIAA 88-0414, 1988.

Massey, S.J. and Abdol-Hamid, K.S., "Enhancement and Validation of PAB3D for Unsteady Aerodynamics," AIAA 2003-1235, 2003.

Melson, N.D., Sanetrik, M.D. and Atkins, H.L., "Time-Accurate Navier-Stokes Calculations with Multigrid Accelerations," 6th Cooper Mountain Conference on Multigrid Methods, 1993.

Mulas, M., Chibbaro, S., Delussu, G., Di Piazza, I. and Talice, M. "Efficient Parallel Computations of Flows of Arbitrary Fluids for All Regimes of Reynolds, Mach and Grashoff Numbers," International Journal of Numerical Methods for Heat & Fluid Flow, 12, 637-657, 2002.

Rizzi, A., Eliasson, P., Lindbland, I., Hirsch, C., Lacor, C. and Haeuser, J., "The Engineering of Multiblock/Multigrid Software for Navier-Stokes Flows on Structured Meshes," Computers & Fluids, 22, 341-367, 1993.

Rogers, S.E. and Kwak, D., "Upwind Differencing Scheme for the Time-accurate Incompressible Navier-Stokes Equations," AIAA Journal, 28, 253-262, 1990.

Roshko, A., "On the Development of Turbulent Wakes from Vortex Streets," NACA Report 1191, 1954.

Schlichting, H., "Boundary-Layer Theory," McGraw-Hill, New York, 1979.

Venkatakrishnan, V. and Mavriplis, D.J., "Implicit Method for the Computation of Unsteady Flows on Unstructured Grids," Journal of Computational Physics, 127, 380-397, 1996.

Vatsa V.N. and Turkel E., "Choice of Variables and Preconditioning for Time Dependent Problems," AIAA 2003-3692, 2003.

Vatsa V.N. and Turkel E., "Assessment of Local Preconditioners for Steady State and Time Dependent Flows," AIAA 2004-2134, 2004.

Weiss, J. and Smith, W.A., "Preconditioning Applied to Variable and Constant Density Flows," AIAA Journal, 33, 2050-2057, 1995.

Wille, R., "Karman Vortex Streets," Advances in Applied Mechanics, 6, 273-287, Academic, New York, 1960.